# Electron relaxation times due to the deformation-potential interaction of electrons with confined acoustic phonons in a free-standing quantum well

N. Bannov, V. Aristov, and V. Mitin
*Department of Electrical and Computer Engineering, Wayne State University, Detroit, Michigan 48202*

M. A. Stroscio
*U.S. Army Research Office, P.O. Box 12211, Research Triangle Park, North Carolina 27709-2211*
(Received 28 June 1994; revised manuscript received 6 October 1994)

The confined acoustic phonons in free-standing quantum wells are considered in detail. The Hamiltonian describing interactions of the confined acoustic phonons with electrons in the approximation of the deformation potential and the corresponding electron transition probability density are derived. They are used to analyze the electron scattering times (inverse scattering rate, momentum relaxation time, and the energy relaxation time) in the test-particle approximation as well as in the kinetic approximation. It is shown that the first dilatational mode makes the main contribution to electron scattering in the lowest electron subband. The contribution of the zeroth mode and the second mode are also essential while the modes of higher order are insignificant. Our analysis is performed for both nondegenerate and degenerate electron gases. It is shown that electron scattering by confined acoustic phonons interacting through the deformation potential is substantially suppressed up to the electron energies corresponding to the energy of the first dilatational mode.

## I. INTRODUCTION

Modern microfabrication techniques have allowed the creation of free-standing quantum nanostructures which have attracted considerable attention and have been studied by several research groups. These structures are, in fact, solid plates (slabs) or rods (bars) connected to a solid substrate by a side of the smallest cross section. The major feature of free-standing structures is that the smallest dimensions of the structures may be as small as a few interatomic distances. This attribute gives rise to interesting physical phenomena and opens many possibilities for applications. First of all, the electrons (holes) in these structures are quantized. In fact, free-standing structures represent waveguides for electron waves which have features substantially different from more conventional quantum structures. Such waveguides may have very high potential-energy barriers for electrons, so effects related to hot but quantized electrons are possible. The phonon subsystem will also undergo significant modification and quantization of the acoustic phonon spectrum in a way similar to the electron quantization should occur.

Free-standing nanostructures have been fabricated in several laboratories. Free-standing quantum wells (FSQW's) made of various metals, such as Al, Ag, and Au had been prepared by electron-beam evaporation or molecular-beam epitaxy on a cleaved NaCl substrate and by subsequently dissolving the substrate.[1,2] The thicknesses of the films were as thin as 200 Å and typical areas of the surfaces were roughly 1 $mm^2$. Semiconductor GaAs and $In_xGa_{1-x}As$ FSQW's have been fabricated from spatially and compositionally modulated superlattices using standard lithographic techniques and selective etching.[3] In those structures FSQW's were suspended between two support posts and the quantum wells were parallel to the surface of the substrate, so the FSQW's remain as bridges. Such structures had reproducible well widths from 80 to 200 Å. The typical in-plane sizes of the FSQW's were $2.5 \times 0.25$ $\mu m^2$.

Results of successful fabrication of free-standing quantum wires (FSQWI's) and free-standing quantum dots are reported in Refs. 4–8; additional references are given in the review of Ref. 4. There are basically two different approaches to FSQWI fabrication. In one of them the FSQWI's are prepared in a manner similar to that used for FSQW preparation with the difference that the widths of such FSQW's are small and constitute only several thicknesses; hence such quantum structures may be considered as FSQWI's.[5] This method had been used to make InAs FSQWI's with widths of 2000–7000 Å and a thickness of 150 Å. In another approach very long GaAs, InAs, and Si whiskers were grown on a GaAs substrate by metal-organic epitaxy.[4,6,9] Quantum dots were obtained by reactive ion etching whiskers in a mixture of $CH_4$ and $H_2$.[7,8] The whiskers were directed along the $\langle 111 \rangle$ direction of the GaAs substrate, whatever the substrate orientation, and had typical lengths of 1 to 5 $\mu$m and diameters of 100 to 2000 Å.

There are several possible applications of the free-standing structures. They may be used for probing the local properties of solids and there are several works where such possibilities were demonstrated.[1,2] Free-standing quantum structures may find applications as very sensitive sensors of forces or displacements in ways similar to those used for thin film sensors,[10] and there exists a variety of potential uses of free-standing structures for electronic and photonic applications, e.g., as low voltage field emitters, light emitting devices, and

 

mirrors for optical resonators.[4,8,11,12] Reference 6 reports work in which the GaAs FSQWI's (whiskers) were grown with built-in $p$-$n$ junctions and Ohmic contacts were fabricated at both sides of the structures. The photoemission spectra as well as the photoluminescence spectra were studied for these FSQWI's. The photoemission spectra displayed redshifts which were not observed in bulk structures grown in the same conditions. A satisfactory explanation of this phenomenon has not been found. The photoluminescence spectra revealed a strong dependence on the orientation of the excitation light polarization with respect to the FSQW's axes. Si FSQWI's illuminated with green light emit red light and this effect may be used in Si based optoelectronics.[9] Optical and transport properties of the FSQWI's were studied theoretically in Refs. 13 and 14, respectively.

In this paper we will concentrate our main attention on physical phenomena related to acoustic phonons in free-standing quantum wells. The quantization of the acoustic phonon spectrum results in modifications of the acoustic phonon interactions with electrons and photons and manifests itself in electrical and optical measurements. The spectra of the acoustic phonons in opaque metal FSQW's were investigated in Refs. 1 and 2. The authors claimed that the Brillouin light scattering technique which they used would work to detect any acoustical mode which produces undulations at the surface. Acoustic phonon confinement may also take place in quantum wells and quantum wires lying on the substrate or buried in the substrate. Quantized acoustic phonons were observed even in conventional AlAs-GaAs-AlAs quantum wells by the photothermal luminescence spectroscopy method.[15] The conductance of AuPd quantum films and wires with widths of 200 Å made on a silicon substrate has also been studied.[16,17] The variation in the conductance as a function of the applied electric field has periodic peaks which authors have attributed to the electron interactions with confined acoustic phonons.

To describe quantitatively electron transport and optical properties of the quantum structures it is necessary to consider all of the acoustic phonon modes, their spectra, and their interactions with electrons and photons. Detailed understanding of confined acoustic phonons in quantum structures and their spectra may also be significant for some of the nondestructive diagnostic methods for microstructures where propagation of the acoustic phonons is employed.[18–20]

While there is an extensive literature on acoustic modes in acoustical waveguides, resonators, and related structures,[21,22] there are relatively few works considering this problem in a context of nanoscale structures.[23–36] In Refs. 23–27 acoustic modes in systems with two interfaces were investigated and attention was drawn primarily to the modes localized between the interfaces. The peculiarities of acoustic phonon modes due to planar defects have also been considered;[29,30] it is shown that a few monolayers of different material[30] or even a built-in electron sheet, interacting with phonons through the deformation potential,[29] may result in localization of some acoustic modes on the planar defect. A number of articles[31–33] have been devoted to one-dimensional acoustical phonons in cylindrical free-standing quantum wires and their interactions with electrons. The similar problems for FSQW's are considered in Refs. 34 and 35 and for FSQWI's of rectangular cross-section in Refs. 36 and 37.

In the following sections we will consider the acoustic modes in FSQW's and analyze the acoustic phonon spectrum. Then we will consider electron scattering by confined acoustic phonons interacting through the deformation potential. The electron relaxation times due to this type of interaction will be obtained in the test-particle approximation as well as in the kinetic approximation for both nondegenerate and degenerate electron gases. We will use the first-order perturbation theory to determine the electron-phonon scattering rates. Though the effects of higher order such as a renormalization of the acoustic phonon spectrum due to phonon interactions with electrons are observable in a two-dimensional (2D) electron gas, they are not significant for the electron concentrations typical for semiconductor 2D structures;[29] therefore, we will not take them into account. The acoustical modes in a solid slab and their spectrum are known from the theory of acoustics; however, we have to give the appropriate expressions for modes and discuss their peculiarities to provide fundamentals for consideration of electron-phonon interactions. Moreover, the acoustic modes have to be normalized to introduce the acoustic phonons and this problem has not been solved in the field of acoustics. This is one more reason to consider the acoustic phonon modes in detail.

## II. EIGENMODES IN FREE-STANDING QUANTUM WELL

### A. Basic equations

We will consider the acoustic modes in FSQW's neglecting the distortion of acoustic vibrations resulting from contact with the solid substrate. This imposes restrictions on the in-plane wavelength, which should be shorter than the characteristic in-plane size of the solid slab. Small elastic vibrations of a solid slab can be described by a vector of relative displacement $\mathbf{u} = \mathbf{u}(\mathbf{r}, t)$. The Lagrangian $L$ of an isotropic continuous medium can be expressed in terms of vibrations as (see, for example, Ref. 38)

$$L = \frac{1}{2}\int [\rho \dot{\mathbf{u}}^2 - \lambda u_{i,i}^2 - 2\mu u_{i,k}^2]\, d\mathbf{r} \,, \tag{1}$$

where $\rho$ is the density of semiconductor, $\lambda, \mu$ are the Lamè constants, $u_{i,j}$ is the strain tensor,

$$u_{i,j} = \frac{1}{2}\left(\frac{\partial u_i}{\partial r_j} + \frac{\partial u_j}{\partial r_i}\right) ,$$

and a dot over $\mathbf{u}$ denotes differentiation with respect to time. The sum is assumed to be taken over repeated subscripts. Equations of motion of elastic continua described by (1) follow from the principle of the least action and have the form

$$\rho \frac{\partial^2 u_\alpha}{\partial t^2} = \frac{\partial \sigma_{\alpha,j}}{\partial r_j}, \tag{2}$$

where $\sigma_{i,j}$ is the stress tensor

$$\sigma_{i,j} = \lambda\ u_{k,k}\ \delta_{i,j} + 2\mu\ u_{i,j}\ ,$$

and $\delta_{i,j}$ is the Kronecker delta. Equation (2) can be rewritten in vector form as

$$\frac{\partial^2 \mathbf{u}}{\partial t^2} = s_t^2\ \nabla^2 \mathbf{u} + (s_l^2 - s_t^2)\ \text{grad div}\ \mathbf{u}\ , \tag{3}$$

where $s_l = (\lambda + 2\mu)/\rho$ and $s_t = \mu/\rho$ are the velocities of longitudinal and transverse acoustic waves in bulk semiconductors. The boundary conditions on the free surface of the slab imply that the components of the stress tensor corresponding to the normal direction to the surface vanish. If we specify the coordinate system (which we will use throughout this paper) in such a way that the axis $z$ is perpendicular to the semiconductor slab and the surfaces of the slab have coordinates $z = \pm(a/2)$, where $a$ is the width of the slab, the boundary conditions take the form $\sigma_{x,z} = \sigma_{y,z} = \sigma_{z,z} = 0$ at $z = \pm(a/2)$; accordingly, in terms of components of the displacement vector, it follows that

$$\begin{aligned} \sigma_{x,z} &= \mu \left(\tfrac{\partial u_x}{\partial z} + \tfrac{\partial u_z}{\partial x}\right) = 0\ , \\ \sigma_{y,z} &= \mu \left(\tfrac{\partial u_y}{\partial z} + \tfrac{\partial u_z}{\partial y}\right) = 0\ , \\ \sigma_{z,z} &= \lambda\ \text{div}\,\mathbf{u} + 2\,\mu\ \tfrac{\partial u_z}{\partial z} = 0\ , \end{aligned} \tag{4}$$

at $z = \pm(a/2)$. Our goal is to find eigenmodes for acoustic vibrations defined by Eqs. (3) and (5). We will look for solutions in the following form:

$$\mathbf{u}(\mathbf{r},t) = \sum_n \int \mathbf{u}_n(\mathbf{q}_\parallel, z)\ \exp(i\mathbf{q}_\parallel \cdot \mathbf{r}_\parallel - i\omega_n t)\ \frac{d\mathbf{q}_\parallel}{(2\pi)^2}\ ,$$

where $\mathbf{r}_\parallel$ is the coordinate vector in the $(x,y)$ plane, $\omega_n$ is the set of frequencies of vibrations. From (3) we can obtain the set of equations for eigenmodes, $\mathbf{u}_n(\mathbf{q}_\parallel, z)$, and eigenfrequencies, $\omega_n$. This may be conveniently done if we direct the axis $x$ of the coordinate system along vector $\mathbf{q}_\parallel$, so that $\mathbf{q}_\parallel = (q_x, 0)$. Then the eigenvalue problem takes the form

$$\mathcal{D}\ \mathbf{u}_n(\mathbf{q}_\parallel, z) = -\omega_n^2 \mathbf{u}_n(\mathbf{q}_\parallel, z)\ , \tag{5}$$

where $\mathcal{D}$ is the matrix differential operator,

$$\mathcal{D} = \begin{bmatrix} s_t^2 \frac{d^2}{dz^2} - s_l^2 q_x^2 & 0 & (s_l^2 - s_t^2) i q_x \frac{d}{dz} \\ 0 & s_t^2 \frac{d^2}{dz^2} - s_t^2 q_x^2 & 0 \\ (s_l^2 - s_t^2) i q_x \frac{d}{dz} & 0 & s_l^2 \frac{d^2}{dz^2} - s_t^2 q_x^2 \end{bmatrix}. \tag{6}$$

The boundary conditions (5) become

$$\frac{du_x}{dz} = -iq_x u_z\ , \quad \frac{du_y}{dz} = 0\ , \quad \frac{du_z}{dz} = -iq_x \frac{s_l^2 - 2s_t^2}{s_l^2} u_x \tag{7}$$

at $z = \pm(a/2)$. It can be proved straightforwardly that the operator $\mathcal{D}$ of the eigenvalue problem (5)–(7) is Hermitian, so the eigenfunctions, $\mathbf{u}_n(\mathbf{q}_\parallel, z)$, corresponding to nondegenerate eigenfrequencies, $\omega_n$, are orthogonal. We can also orthogonalize eigenfunctions corresponding to equal eigenfrequencies using the Schmidt orthogonalization procedure. We will use $\mathbf{w}$ instead of $\mathbf{u}$ to denote the orthonormal set of eigenvectors, $\mathbf{w}_n(\mathbf{q}_\parallel, z)$, of problem (5)–(7), for which

$$\int \mathbf{w}_n^\dagger(\mathbf{q}_\parallel, z)\mathbf{w}_m(\mathbf{q}_\parallel, z)\ dz = \delta_{n,m}\ . \tag{8}$$

### B. Confined eigenmodes

The eigenvalue problem of Eqs. (5)–(7) can be solved through the introduction of vector and scalar mechanical potentials which define the vector of relative displacement.[21,22] The solution of this problem is known from acoustics[21,22] and we will use acoustical terminology to identify eigenmodes. What has not been done in the field of acoustics is the normalization of eigenmodes (this is essentially a quantum mechanical problem); in addition, interactions of confined modes with electrons have not been investigated. A major feature of the confined modes is the quantization of the phonon wave vector in the $z$ direction, i.e., the $z$ components of the confined mode wave vectors, $q_z$, take only some discrete set of values at each particular in-plane wave vector, $\mathbf{q}_\parallel$. There are three different types of confined acoustic modes: shear waves, dilatational waves, and flexural waves. They are characterized by their distinctive symmetries.

#### *1. Shear waves*

These waves have only one nonzero component which is perpendicular to the direction of wave propagation and lies in the plane of the quantum well: $\mathbf{u}_n(\mathbf{q}_\parallel, z) = (0, u_y, 0)$ , where

$$u_y = \begin{cases} \cos(q_{z,n}\ z) & \text{if } n = 0,2,4,... \\ \sin(q_{z,n}\ z) & \text{if } n = 1,3,5,..., \end{cases} \tag{9}$$

$q_{z,n} = (\pi n/a)$ . The dispersion relation for shear waves is

$$\omega_n = s_t \sqrt{q_{z,n}^2 + q_x^2}\ .$$

These modes are similar to the transverse modes in bulk semiconductors and the $q_z$ quantization is based on the simple rule stating that an integer number of half wavelengths fits in a semiconductor slab of width $a$ .

#### *2. Dilatational waves*

These waves are also called symmetric waves (in respect to the midplane) and have two nonzero components: $\mathbf{u}_n(\mathbf{q}_\parallel, z) = (u_x, 0, u_z)$ , where

$$u_x = iq_x\left[(q_x^2 - q_t^2)\sin\frac{q_t a}{2}\cos q_l z + 2q_l q_t \sin\frac{q_l a}{2}\cos q_t z\right], \quad (10)$$

$$u_z = q_l\left[-(q_x^2 - q_t^2)\sin\frac{q_t a}{2}\sin q_l z + 2q_x^2 \sin\frac{q_l a}{2}\sin q_t z\right]. \quad (11)$$

The parameters $q_l, q_t$ are determined from the system of two algebraic equations,

$$\frac{\tan(q_t a/2)}{\tan(q_l a/2)} = -\frac{4q_x^2 q_l q_t}{(q_x^2 - q_t^2)^2}, \quad (12)$$

$$s_l^2\,(q_x^2 + q_l^2) = s_t^2\,(q_x^2 + q_t^2)\,. \quad (13)$$

Equations (12) and (13) have many solutions for $q_l$ and $q_t$ at each particular $q_x$,[21] and we label them by an additional index $n$: $q_{l,n}$, $q_{t,n}$. These solutions are either real or pure imaginary depending on $q_x$ and $n$. We will use term *branches* of solutions to denote functions $q_{l,n}(q_x)$, $q_{t,n}(q_x)$, graphs of which are continuous single-connected curves. The frequencies of the dilatational waves are given by

$$\omega_n = s_l\sqrt{q_x^2 + q_{l,n}^2} = s_t\sqrt{q_x^2 + q_{t,n}^2}\,. \quad (14)$$

It is necessary to employ a numerical approach to solve Eqs. (12) and (13).

The results of the numerical solution of Eqs. (12) and (13) are represented in Fig. 1. The only material parameter which affects the solutions is the ratio of $s_l/s_t$. The numerical analysis was done for a GaAs slab with $s_l = 5.7 \times 10^5$ cm/s and $s_t = 3.35 \times 10^5$ cm/s. The values of $q_l$ and $q_t$ above the abscissa are real and below the abscissa are pure imaginary. The dispersion relation for dilatational phonons, calculated for a 100 Å width free-standing quantum well is given in Fig. 2.

The lowest dilatational mode has a linear dispersion relation for small $q_x$. An important peculiarity of this mode is the pure imaginary value of $q_l$, while the value of $q_t$ is real. This means that the lowest dilatational mode contains terms $\sin(q_t z)$ and $\cos(q_t z)$ which are extended throughout the width of the slab as well as terms $\sin(q_l z) = i\sinh(|q_l|z)$ and $\cos(q_l z) = \cosh(|q_l|z)$ which are localized at the surfaces of the slab [see Eqs. (10) and (11)].

### 3. *Flexural waves*

The last type of wave in quantum wells are flexural or antisymmetric waves. Flexural waves have two nonzero components: $\mathbf{u}_n(\mathbf{q}_\parallel, z) = (u_x, 0, u_z)$,

$$u_x = iq_x\left[(q_x^2 - q_t^2)\cos\frac{q_t a}{2}\sin q_l z + 2q_l q_t \cos\frac{q_l a}{2}\sin q_t z\right], \quad (15)$$

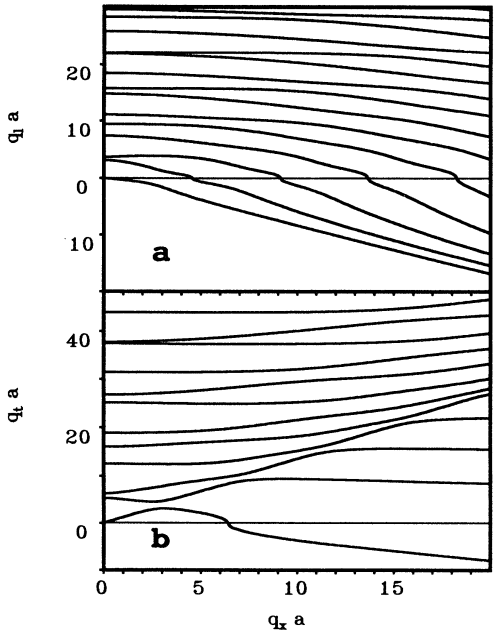


FIG. 1. Parameters $q_l$ (a) and $q_t$ (b) as functions of the in-plane wave vector, $q_x$, for dilatational modes. Several of the lowest order branches are depicted. The values of $q_l$ and $q_t$ above the abscissa are real; the values of $q_l$ and $q_t$ below the abscissa are pure imaginary.

$$u_z = q_l\left[(q_x^2 - q_t^2)\cos\frac{q_t a}{2}\cos q_l z - 2q_x^2 \cos\frac{q_l a}{2}\cos q_t z\right], \quad (16)$$

where $q_l, q_t$ are determined from the solution of the transcendental equation,

$$\frac{\tan(q_l a/2)}{\tan(q_t a/2)} = -\frac{4q_x^2 q_l q_t}{(q_x^2 - q_t^2)^2}, \quad (17)$$

and Eq. (13). The system of algebraic equations (13) and (17) prescribing the quantization rule for flexural

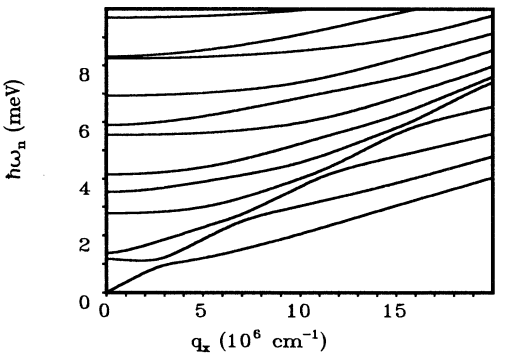


FIG. 2. The dispersion relation for dilatational modes in GaAs FSQW of width 100 Å. Several branches of the lowest order are depicted.

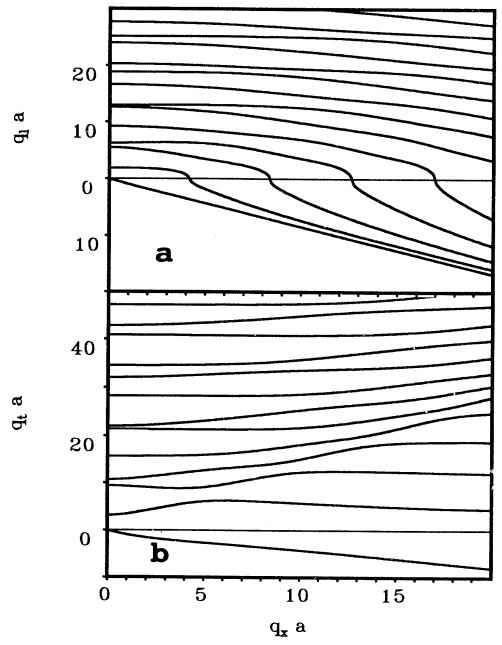


FIG. 3. Parameters $q_l$ (a) and $q_t$ (b) as functions of in-plane wave vector, $q_x$, for flexural modes. Several of the lowest order branches are depicted. The values of $q_l$ and $q_t$ above the abscissa are real; the values of $q_l$ and $q_t$ below the abscissa are pure imaginary.

waves also has many solutions for $q_l$ and $q_t$ at each particular $q_x$,[21] and we again use an additional index $n$ to number them: $q_{l,n}$, $q_{t,n}$. Solutions $q_l$ and $q_t$ may be either real numbers or pure imaginary numbers for a given set $q_x$ and $n$. The dispersion relation for flexural waves coincides with the relation for dilatational waves (14) (this does not result in the coincidence of frequencies because the solutions for $q_{l,n}$ and $q_{t,n}$ are different for dilatational and flexural modes).

We have solved Eqs. (17) and (13) numerically and results are shown in Fig. 3. Again we used the convention that values of $q_l$ and $q_t$ above the abscissa axis are real and those below the abscissa axis are pure imaginary. Calculations are performed for a GaAs slab. The dispersion relation for flexural phonons in a 100 Å GaAs quantum well is shown in Fig. 4.

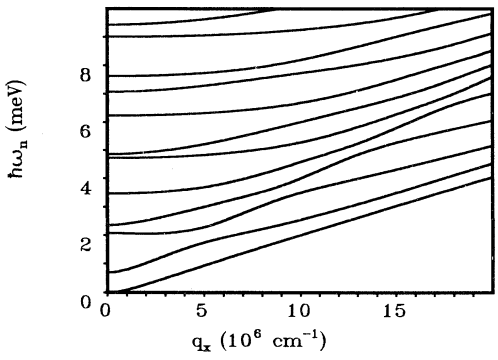


FIG. 4. The dispersion relation for flexural modes in GaAs FSQW of width 100 Å. Several branches of the lowest order are depicted.

The most interesting feature of the dispersion relation for the flexural mode of the lowest order is the quadratic dependence of frequency on the magnitude of the in-plane wave vector. This unusual dependence is due to the fact that for this mode both $q_l$ and $q_t$ are pure imaginary numbers, thus the acoustic vibrations have essentially surface bound character and their amplitudes decrease exponentially from the surface to the interior of the slab [see Eqs. (15) and (16)].

### C. Normalization constants

Now we introduce the normalization constants $F_{s,n}$, $F_{d,n}$, and $F_{f,n}$, such that $\mathbf{w}_n = F_{s,n}\mathbf{u}_n$ for shear waves, $\mathbf{w}_n = F_{d,n}\mathbf{u}_n$ for dilatational waves, and $\mathbf{w}_n = F_{f,n}\mathbf{u}_n$ for flexural waves. Functions $\mathbf{u}_n$ are determined by Eqs. (9) for shear waves, by Eqs. (10) and (11) for dilatational waves, and by Eqs. (15) and (16) for flexural waves. Functions $\mathbf{w}_n$ satisfy the orthonormality conditions (8). These normalization constants $F_{s,n}$, $F_{d,n}$, and $F_{f,n}$ are required to correctly determine the electron-phonon interaction Hamiltonians. They may be determined straightforwardly; however, explicit expressions for these normalization constants are quite awkward and, accordingly, we refer the reader to Ref. 34, where we have given the explicit formulas.

## III. ELECTRON-CONFINED ACOUSTIC PHONON SCATTERING

The confined acoustic modes may be reformulated in terms of phonons in a standard manner using either the Lagrangian formalism (as it has been done for confined acoustic modes in Ref. 34) or the principle that each normal mode carries energy $\hbar\omega_n$ (see, e.g., Ref. 31). The operator for the relative displacement, $\mathbf{u}(\mathbf{r})$, may be expressed through the eigenmodes $\mathbf{w}_n(\mathbf{q}_\parallel, z)$ and the corresponding creation and annihilation operators, $c_n(\mathbf{q}_\parallel)$ and $c_n^\dagger(\mathbf{q}_\parallel)$, by the formula[34]

$$\mathbf{u}(\mathbf{r}) = \sum_{\mathbf{q}_\parallel, n} \sqrt{\frac{\hbar}{2\mathcal{A}\rho\omega_n(\mathbf{q}_\parallel)}}\,[c_n(\mathbf{q}_\parallel) + c_n^\dagger(-\mathbf{q}_\parallel)] \times \mathbf{w}_n(\mathbf{q}_\parallel, z)\, e^{i\mathbf{q}_\parallel\cdot\mathbf{r}_\parallel}. \tag{18}$$

### A. Deformation-potential interaction

We will use the standard form of the Hamiltonian of the electron-acoustic phonon interactions through the deformation potential (see, for example, Ref. 39)

$$H_{\rm def} = E_a \ \mathrm{div}\ \mathbf{u}(\mathbf{r}), \tag{19}$$

where $E_a$ is a deformation-potential coupling constant. From Eqs. (18) and (19) it follows that

$$H_{\rm def} = \sum_{\mathbf{q}_\parallel, n} e^{i\mathbf{q}_\parallel \cdot \mathbf{r}_\parallel} \, \Gamma(\mathbf{q}_\parallel, n, z) \, \left[ c_n(\mathbf{q}_\parallel) + c_n^\dagger(-\mathbf{q}_\parallel) \right] , \tag{20}$$

where

$$\Gamma(\mathbf{q}_\parallel, n, z) = \sqrt{\frac{\hbar E_a^2}{2\mathcal{A}\rho\omega_n(\mathbf{q}_\parallel)}} \left( i\mathbf{q}_\parallel \cdot \mathbf{w}_n(\mathbf{q}_\parallel, z) + \frac{\partial w_{nz}(\mathbf{q}_\parallel, z)}{\partial z} \right). \tag{21}$$

It is obvious for shear waves that $\Gamma_s(\mathbf{q}_\parallel, n) = 0$. Hence, shear waves do not interact with electrons; this is in line with the fact that transverse phonons in bulk isotropic solids do not interact with electrons through the deformation potential. On the contrary, both dilatational and flexural waves contribute to the Hamiltonian for electron-acoustic phonon scattering. Accordingly, the functions $\Gamma_d$ and $\Gamma_f$, describing the intensity of the electron interactions with dilatational and flexural waves are given by

$$\Gamma_d(\mathbf{q}_\parallel, n, z) = F_{d,n} \sqrt{\frac{\hbar E_a^2}{2\,\mathcal{A}\,\rho\,\omega_n(\mathbf{q}_\parallel)}} \times \left[ \left(q_{t,n}^2 - {q_x}^2\right) \left(q_{l,n}^2 + {q_x}^2\right) \times \sin\left(\frac{a\,q_{t,n}}{2}\right) \cos(q_{l,n}\,z) \right], \tag{22}$$

$$\Gamma_f(\mathbf{q}_\parallel, n, z) = F_{f,n} \sqrt{\frac{\hbar E_a^2}{2\,\mathcal{A}\,\rho\,\omega_n(\mathbf{q}_\parallel)}} \times \left[ \left(q_{t,n}^2 - {q_x}^2\right) \left(q_{l,n}^2 + {q_x}^2\right) \times \cos\left(\frac{a\,q_{t,n}}{2}\right) \sin(q_{l,n}\,z) \right]. \tag{23}$$

From Eqs. (22) and (23) we may see an interesting feature of the functions $\Gamma_d$ and $\Gamma_f$; they depend on the $z$ coordinate as functions $\cos(q_l\,z)$ and $\sin(q_l\,z)$ (obtained from displacements associated with longitudinal vibrations). Additionally, the eigenmodes (10), (11), (15), and (16) also have $\cos(q_t\,z)$ and $\sin(q_t\,z)$ terms which may be associated with transverse vibrations; these transverse terms were canceled in the calculation of functions $\Gamma$ and do not appear in the final results.

Another important property of the functions $\Gamma_d$ and $\Gamma_f$ is their opposite symmetry. The function $\Gamma_d$ is symmetric, but the function $\Gamma_f$ is antisymmetric; this results in substantially different contributions to electron scattering from dilatational and flexural phonons. If the electron potential energy in the FSQW is a symmetric function of the $z$ coordinate, then the electron states may be classified by the symmetry of the electron wave function into symmetric and antisymmetric states. Dilatational phonons will interact only with electrons scattered between two states of the same symmetry while the scattering by flexural phonons will result in the electron transition between two states of the opposite symmetry.

It is interesting to note that there is a significant similarity between the Hamiltonian for electron interactions with confined acoustic phonons and interactions with confined and interface optical phonons (see, for example, Ref. 40). In both cases electrons interact with many phonon modes and spatial dependence of the Hamiltonian in the $z$ direction is a linear combination of either sin and cos functions or sinh and cosh functions (in the case of optical phonons this corresponds to either confined or interface phonons). However, the acoustic phonon energy is a strong function of the quantum number, corresponding to motion transverse to the slab, whereas the optical phonon energy dependence on the value of the similar quantum number is weak.

The deformation potential which we have considered above is the major mechanism of electron-acoustic phonon interactions in FSQW's. Another mechanism of scattering is the piezoelectric potential. The Hamiltonian for it in FSQW's has been obtained in Ref. 34. The ratio of the piezoelectric potential strength to the deformation potential strength is equal to $(\frac{e e_{14}}{E_a q})^2$, where $e_{14}$ is the piezoelectric constant and $q$ is the wave vector of the participating in the scattering phonon. In bulk semiconductors the piezoelectric scattering becomes stronger than the deformation-potential scattering at low lattice temperatures and in low electric fields because electrons are scattered mainly by acoustic phonons with small $q$. In FSQW's there is a lower limit for $q$ which is equal to $\pi/a$ due to the $q_z$ component quantization. For this reason the deformation-potential scattering dominates in FSQW's.

### B. Transition probability density

The electron wave functions in a free-standing quantum well have the form

$$\psi_{\mathbf{k}_\parallel, n} = \exp(i\mathbf{k}_\parallel \cdot \mathbf{r}_\parallel) \, \varphi_n(z) \, / \, \sqrt{L_x L_y} \, ,$$

where $L_x$ and $L_y$ are the in-plane sizes of the 2D structure ($L_x\,L_y = \mathcal{A}$), $n$ is a discrete index corresponding to the quantization in the $z$ direction (electron subband number), and functions $\varphi_n(z)$ are eigenfunctions of the 1D Schrödinger equation. We assume that they are orthogonal, so that $\langle \varphi_n \mid \varphi_m \rangle = \delta_{n,m}$. The electron spectrum has the form $\varepsilon = \varepsilon_n + \hbar^2 {k_\parallel}^2 / 2\,m^*$. The acoustic phonons are characterized by the in-plane wave vector $\mathbf{q}_\parallel$, the mode number $m$, and the symmetry $\alpha$.

We are considering the electron-phonon interactions though the deformation potential which may be represented by the scheme

$$(\mathbf{k}_\parallel, n) \pm (\mathbf{q}_\parallel, m, \alpha) \longrightarrow \left(\mathbf{k}'_\parallel, n'\right).$$

An electron with quantum numbers $(\mathbf{k}_\parallel, n)$ absorbs (up-

per sign) or emits (lower sign) acoustic phonon with quantum numbers $(\mathbf{q}_\parallel, m, \alpha)$ and becomes an electron with quantum numbers $(\mathbf{k}'_\parallel, n')$.

The probability density for the transition from the initial state $i$ to the final state $f$ is given by the Fermi golden rule

$$W_{i\to f} = \frac{2\pi}{\hbar}\left|\langle f \mid H_{\rm def} \mid i\rangle\right|^2 \delta(\varepsilon_f - \varepsilon_i)\,, \tag{24}$$

where $\varepsilon_i$ and $\varepsilon_f$ are the energies of the electron-phonon system before and after scattering. Simplifying the integral (24) we may obtain

$$W^{\left\{\begin{smallmatrix}\rm ab\\ \rm em\end{smallmatrix}\right\}}_{\mathbf{k}_\parallel, n\to\mathbf{k}'_\parallel, n'} = \frac{\pi E_a^2 \left(n^\alpha_{\mathbf{q}_\parallel, m} + \frac{1}{2} \mp \frac{1}{2}\right) \mid F_{\alpha,m} \mid^2 \left(q^2_{t,m} - q_x{}^2\right)^2 \left(q^2_{l,m} + q_x{}^2\right)^2}{\mathcal{A}\,\rho\,\omega^{(\alpha)}_m(\mathbf{q}_\parallel)}$$
$$\times\, {\rm tsc}^2_\alpha\left(\frac{a\,q_{t,m}}{2}\right) \mathcal{G}(n', n, \alpha, q_{l,m})\, \delta_{\mathbf{k}_\parallel \pm \mathbf{q}_\parallel, \mathbf{k}'_\parallel}\, \delta[\varepsilon \pm \hbar\omega^{(\alpha)}_m(\mathbf{q}_\parallel) - \varepsilon']\,, \tag{25}$$

where function ${\rm tsc}_\alpha = \sin$ if $\alpha =$ (dilatational) and function ${\rm tsc}_\alpha = \cos$ if $\alpha =$ (flexural), upper signs are for phonon emission, and lower signs are for absorption. The parameters $q_{l,m}$ and $q_{t,m}$, in fact, depend on the type of mode (dilatational or flexural); we have simplified notations and omitted $\alpha$. The overlap integral, $\mathcal{G}(n', n, \alpha, q)$, is given by the formula

$$\mathcal{G}(n', n, \alpha, q) = \left|\int_{-a/2}^{a/2} dz\; \varphi^*_{n'}(z)\, \varphi_n(z)\, {\rm tcs}_\alpha(q\,z)\right|^2$$

where function ${\rm tcs}_\alpha = \cos$ if $\alpha =$ dilatational and function ${\rm tcs}_\alpha = \sin$ if $\alpha =$ (flexural). The argument $q$ takes both real and pure imaginary values.

If we take electron wave functions for a rectangular infinitely deep quantum well, the overlap integral may be calculated analytically. For even $n + n'$ and $\alpha =$ (dilatational) and also for odd $n + n'$ and $\alpha =$ (flexural) it takes the form

$$\mathcal{G}(n', n, \alpha, q) = \frac{32\,(n'\,n\,\tilde{q})^2\,[\,1 - (-1)^{n+n'}\cos\pi\tilde{q}\,]}{\pi^2\,[\,\tilde{q}^4 - 2(n'^2 + n^2)\tilde{q}^2 + (n^2 - n'^2)^2\,]^2}\,,$$

where $\tilde{q} = a\,q/\pi$ , if $q$ is real. If $q$ is a pure imaginary number, the overlap integral is equal to

$$\mathcal{G}(n', n, \alpha, q) = \frac{32\,(n'\,n\,\tilde{p})^2\,[\,-(-1)^{n+n'} + \cosh\pi\tilde{p}\,]}{\pi^2\,[\,\tilde{p}^4 + 2(n'^2 + n^2)\tilde{p}^2 + (n^2 - n'^2)^2\,]^2}\,,$$

where $\tilde{p} = -i\,a\,q/\pi$. If $n + n'$ is an odd number and $\alpha =$ (dilatational) or if $n + n'$ is an even number and $\alpha =$ (flexural) the overlap integral is equal to zero in accordance with the selection rules discussed in Sec. III A.

In the following two sections we will need to take the sums

$$\tau_G^{-1} = \sum_{n', \mathbf{k}'_\parallel, \alpha, m, \mathbf{q}_\parallel, \beta} W^\beta_{\mathbf{k}_\parallel, n\to\mathbf{k}'_\parallel, n'}\; G\,, \tag{26}$$

where $\beta$ is used to denote either *absorption* or *emission*, and $G$ is some given function which may depend on all variables over which we take the sum. We will use functions $G$, such that $\tau_G^{-1}$ denotes either the scattering rate, or the momentum relaxation rate, or the energy relaxation rate. We will also use $(\tau_G^{\rm ab})^{-1}$ and $(\tau_G^{\rm em})^{-1}$ which are defined in a similar way to $\tau_G^{-1}$ with the only distinction that we sum either only absorption terms or only emission terms. There is an obvious relation between them: $\tau_G^{-1} = (\tau_G^{\rm ab})^{-1} + (\tau_G^{\rm em})^{-1}$. Here we will give a general formula how to calculate the sum (26).

If we employ the formulas for transition probabilities (25) and integrate the $\delta$ function of energy, we will obtain the following result for scattering rates:

$$\left(\tau_G^{\left\{\begin{smallmatrix}\rm ab\\ \rm em\end{smallmatrix}\right\}}\right)^{-1} = \frac{E_a^2\, m}{2\,\pi\,\hbar^2\,\rho\,k_\parallel} \sum_{n', \alpha, m} \sum_i \int_0^\infty dq_\parallel\; \mathcal{F}^{\left\{\begin{smallmatrix}\rm ab\\ \rm em\end{smallmatrix}\right\}}(n',\, n,\, \alpha,\, m,\, q_\parallel)\; G\; \frac{1}{\mid \sin\Psi_i \mid}\,, \tag{27}$$

where

$$\mathcal{F}^{\left\{\begin{smallmatrix}\rm ab\\ \rm em\end{smallmatrix}\right\}}(n',\, n,\, \alpha,\, m,\, q_\parallel) = \frac{\left(n^\alpha_{\mathbf{q}_\parallel, m} + \frac{1}{2} \mp \frac{1}{2}\right) \mid F_{\alpha,m} \mid^2 \left(q^2_{t,m} - q_x{}^2\right)^2 \left(q^2_{l,m} + q_x{}^2\right)^2}{\omega^{(\alpha)}_m(\mathbf{q}_\parallel)} {\rm tsc}^2_\alpha\left(\frac{a\,q_{t,m}}{2}\right)\; \mathcal{G}(n', n, \alpha, q_{l,m})\,,$$

and angles $\Psi_i \in [0,\pi]$ are solutions of the transcendental equation

$$\cos\Psi = \frac{m\,\omega_m^{(\alpha)}(q_\parallel)}{\hbar\,k_\parallel\,q_\parallel} \pm \left(\frac{m\,(\varepsilon_n - \varepsilon_{n'})}{\hbar^2\,k_\parallel\,q_\parallel} - \frac{q_\parallel}{2\,k_\parallel}\right) .$$

Actually, $\Psi$ is the angle between $\mathbf{k}_\parallel$ and $\mathbf{q}_\parallel$. In the transition from Eq. (26) to Eq. (27) we have replaced the summation over a quasidiscrete variable by integration over a corresponding continuous variable. Hereafter we will use summation and integration over quasidiscrete variables interchangeably for the sake of convenience.

## IV. RELAXATION TIMES IN THE TEST-PARTICLE APPROXIMATION

In this section we will use the notation $f_{\mathbf{p}}$ for the electron distribution function. The temporal and the spatial dependence of the distribution function is not important for us and we omit the variables $t$ and $\mathbf{r}$. The variable $\mathbf{p}$ is the electron momentum; however, for the sake of conciseness we assume that this parameter also includes the electron subband number. The collision integral, $S$, accounting for electron scattering by phonons has the form

$$S = \sum_{\mathbf{p}'} [\, W_{\mathbf{p}'\to\mathbf{p}}\, f_{\mathbf{p}'}\,(1-f_{\mathbf{p}}) - W_{\mathbf{p}\to\mathbf{p}'}\, f_{\mathbf{p}}\,(1-f_{\mathbf{p}'})\,] ,$$

where $W_{\mathbf{p}\to\mathbf{p}'}$ is a probability of transition from a quantum state $\mathbf{p}$ to a quantum state $\mathbf{p}'$ per unit time. We will also consider quantities $S_g$, defined as

$$S_g = \sum_{\mathbf{p}} g(\mathbf{p})\, S(\mathbf{p}) ,$$

where $g(\mathbf{p})$ is some function. The principle of the detailed balance states

$$W_{\mathbf{p}'\to\mathbf{p}}\, f^0_{\mathbf{p}'}\,(1-f^0_{\mathbf{p}}) = W_{\mathbf{p}\to\mathbf{p}'}\, f^0_{\mathbf{p}}\,(1-f^0_{\mathbf{p}'}) ,$$

where $f^0_{\mathbf{p}}$ is the equilibrium distribution function (the Fermi function). If we represent the distribution function in the form

$$f_{\mathbf{p}} = f^0_{\mathbf{p}} + \delta f_{\mathbf{p}} ,$$

then the collision integral takes the form

$$S = \sum_{\mathbf{p}'} W_{\mathbf{p}\to\mathbf{p}'} \left[ \frac{f^0_{\mathbf{p}}}{f^0_{\mathbf{p}'}}\delta f_{\mathbf{p}'} - \frac{1-f^0_{\mathbf{p}'}}{1-f^0_{\mathbf{p}}}\delta f_{\mathbf{p}} + \frac{f^0_{\mathbf{p}'} - f^0_{\mathbf{p}}}{f^0_{\mathbf{p}'}\,(1-f^0_{\mathbf{p}})}\delta f_{\mathbf{p}}\delta f_{\mathbf{p}'} \right] , \tag{28}$$

and the quantity $S_g$ takes the form

$$S_g = \sum_{\mathbf{p},\mathbf{p}'} [\, g(\mathbf{p}') - g(\mathbf{p})\,]\, W_{\mathbf{p}\to\mathbf{p}'}\, \frac{1-f^0_{\mathbf{p}'}}{1-f^0_{\mathbf{p}}}\, \delta f_{\mathbf{p}} . \tag{29}$$

The formula for $S_g$ does not contain nonlinear terms because they cancel out.

We define the *electron scattering rate*, $\tau(\mathbf{p})^{-1}$, as the function

$$\tau(\mathbf{p})^{-1} = \sum_{\mathbf{p}'} W_{\mathbf{p}\to\mathbf{p}'}\, \frac{1-f^0_{\mathbf{p}'}}{1-f^0_{\mathbf{p}}} . \tag{30}$$

In accordance with Eq. (28), $\tau(\mathbf{p})^{-1}$ denotes the rate for an electron to escape from a quantum state $\mathbf{p}$ due to scattering if the nonlinear (in respect to $\delta f_{\mathbf{p}}$) term in the collision integral is neglected. In the case of a nondegenerate electron gas $\tau(\mathbf{p})^{-1}$ is the electron scattering probability density integrated over all final states. We will use the electron scattering rate later in this section.

In the test particle approximation $\delta f_{\mathbf{p}} = \delta_{\mathbf{p},\mathbf{p}_0}$ at $t = 0$, where $\mathbf{p}_0$ is a momentum of the test electron. The kinetic equation for $\delta f_{\mathbf{p}}$ has the form

$$\partial\delta f_{\mathbf{p}}/\partial t = S . \tag{31}$$

If we multiply the kinetic equation (31) by $g(\mathbf{p})$ and take sum over $\mathbf{p}$ we obtain

$$\partial g(\mathbf{p}_0)/\partial t = S_g , \tag{32}$$

where the following relation has been used:

$$\sum_{\mathbf{p}} g(\mathbf{p})\,\delta f_{\mathbf{p}} = g(\mathbf{p}_0) .$$

From Eqs. (32) and (29) it follows that the equation for $g(\mathbf{p}_0)$ may be represented in the form

$$\frac{\partial g(\mathbf{p}_0)}{\partial t} = -\frac{g(\mathbf{p}_0)}{\tau_g(\mathbf{p}_0)} , \tag{33}$$

where the relaxation time of the quantity $g$, $\tau_g(\mathbf{p})$, is defined as

$$\tau_g(\mathbf{p})^{-1} = \sum_{\mathbf{p}'} W_{\mathbf{p}\to\mathbf{p}'} \left[1 - \frac{g(\mathbf{p}')}{g(\mathbf{p})}\right] \frac{1-f^0_{\mathbf{p}'}}{1-f^0_{\mathbf{p}}} . \tag{34}$$

This is the basic formula which determines all the relaxation times in the test particle approximation.

*Momentum relaxation time.* In this case $g(\mathbf{p}') = p'\cos\varphi$, where $\varphi$ is the angle between $\mathbf{p}'$ and $\mathbf{p}$,

$$\tau_p(\mathbf{p})^{-1} = \sum_{\mathbf{p}'} W_{\mathbf{p}\to\mathbf{p}'} \left[1 - \frac{p'\cos\varphi}{p}\right] \frac{1-f^0_{\mathbf{p}'}}{1-f^0_{\mathbf{p}}} . \tag{35}$$

*Energy relaxation time.* In this case $g(\mathbf{p}) = \varepsilon$, where $\varepsilon = p^2/2m^*$ is the electron energy,

$$\tau_\varepsilon(\mathbf{p})^{-1} = \sum_{\mathbf{p}'} W_{\mathbf{p}\to\mathbf{p}'} \left[1 - \frac{\varepsilon'}{\varepsilon}\right] \frac{1-f^0_{\mathbf{p}'}}{1-f^0_{\mathbf{p}}} . \tag{36}$$

The formulas (30), (35), and (36) define the scattering time, the momentum relaxation time, and the energy relaxation time of the test electron for any mechanism of scattering. Applied to the electron scattering

by the confined acoustic phonons these formulas specify the functions $G$ which appear in Eqs. (26) and (27). As follows from Eqs. (30), (35), and (36), $G = \frac{1-f^0_{\mathbf{p}'}}{1-f^0_{\mathbf{p}}}$ in the case of the scattering rate, $G = \left[1 - \frac{p' \cos\varphi}{p}\right] \frac{1-f^0_{\mathbf{p}'}}{1-f^0_{\mathbf{p}}}$ in the case of the momentum relaxation time, and $G = \left[1 - \frac{\varepsilon'}{\varepsilon}\right] \frac{1-f^0_{\mathbf{p}'}}{1-f^0_{\mathbf{p}}}$ in the case of the energy relaxation time.

We have computed integrals in (30), (35), and (36) numerically and obtained the electron scattering rates $\tau^{-1}$, $\tau_p^{-1}$, and $\tau_\varepsilon^{-1}$ as functions of energy. Calculations have been performed for GaAs FSQW of width 100 Å and for both nondegenerate and degenerate electron gases in a wide range of the lattice temperatures. In GaAs FSQW of width 100 Å the second electron subband is 168 meV above the first electron subband. Therefore, the population of the second subband may be neglected and we will consider only the lowest electron subband. In the degenerate case we took the Fermi energy, $\varepsilon_F = 50$ meV. This energy corresponds to the electron concentration $n_s = 1.4 \times 10^{12}$ cm$^{-2}$.

The graphs of the functions $\tau^{-1}$, $\tau_p^{-1}$, and $\tau_\varepsilon^{-1}$ for the case of a nondegenerate electron gas and for the lattice temperatures $T = 300, 77$, and 4.2 K are represented in Figs. 5, 6, and 7, correspondingly. The graphs for the

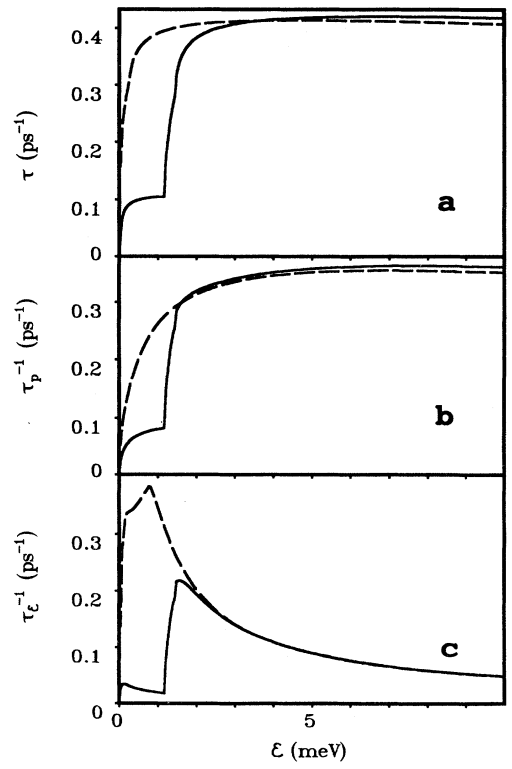


FIG. 5. The electron scattering rate, $\tau^{-1}$ (a), the inverse momentum relaxation time, $\tau_p^{-1}$ (b), and the inverse energy relaxation time, $\tau_\varepsilon^{-1}$ (c) as functions of electron energy. Nondegenerate electron gas, $T = 300$ K, GaAs FSQW of width 100 Å. The solid lines correspond to acoustic phonon emission and the dashed lines correspond to acoustic phonon absorption.

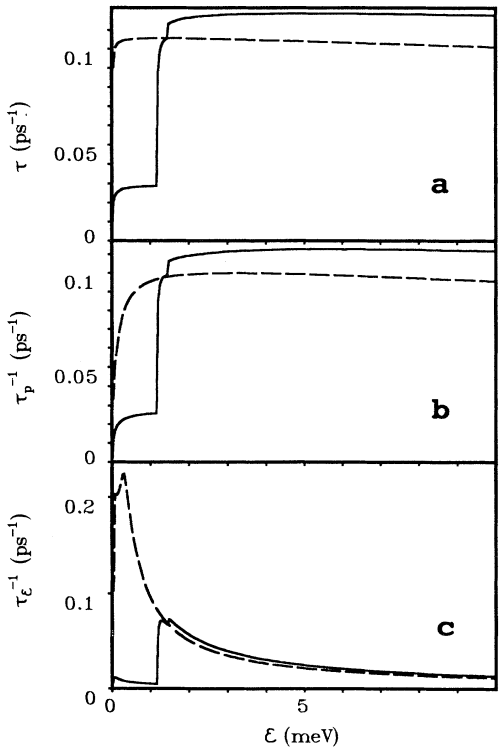


FIG. 6. The electron scattering rate, $\tau^{-1}$ (a), the inverse momentum relaxation time, $\tau_p^{-1}$ (b), and the inverse energy relaxation time, $\tau_\varepsilon^{-1}$ (c) as functions of electron energy. Nondegenerate electron gas, $T = 77$ K, GaAs FSQW of width 100 Å. The solid lines correspond to acoustic phonon emission and the dashed lines correspond to acoustic phonon absorption.

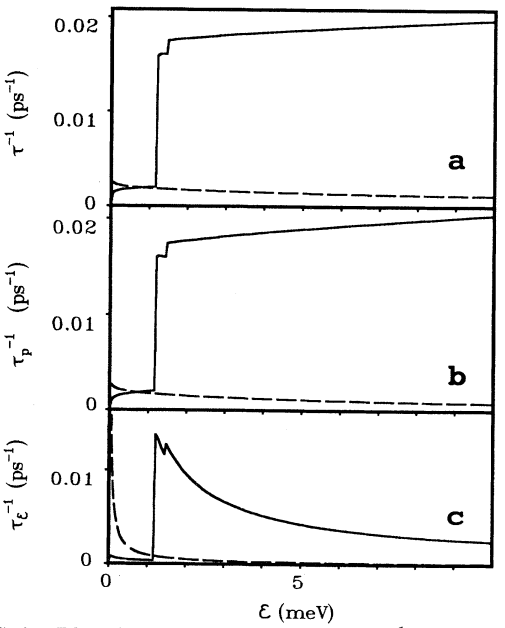


FIG. 7. The electron scattering rate, $\tau^{-1}$ (a), the inverse momentum relaxation time, $\tau_p^{-1}$ (b), and the inverse energy relaxation time, $\tau_\varepsilon^{-1}$ (c) as functions of electron energy. Nondegenerate electron gas, $T = 4.2$ K, GaAs FSQW of width 100 Å. The solid lines correspond to acoustic phonon emission and the dashed lines correspond to acoustic phonon absorption.

relaxation rates corresponding to the degenerate case are depicted in Figs. 8–10 also for the lattice temperatures $T = 300, 77$, and 4.2 K. The solid lines in Figs. 5–10 correspond to acoustic phonon emission and the dashed lines correspond to the acoustic phonon absorption. The quantities $\tau_\varepsilon^{-1}$ for phonon absorption are obviously negative due to the factor $[1 - \varepsilon'/\varepsilon]$; however, to make plots more compact we use the same axes as for the energy relaxation rate corresponding to the phonon emission and plot them as positive functions. An important conclusion we can draw from analyzing these graphs is that the first dilatational mode makes the main contribution to the electron scattering (and to the momentum and energy relaxation); however, contributions of the zeroth and the second dilatational modes are also essential. Modes of higher order may be neglected without losing calculation accuracy. The functions $\tau^{-1}$ and $\tau_p^{-1}$ are very similar; however, $\tau^{-1}$ is slightly larger. This fact will be of use when we do the kinetic analysis of the relaxation times in the next section. At low lattice temperatures where the acoustic phonon absorption is negligible, the acoustic phonon emission is significantly suppressed up to the electron energies corresponding to the energy of the first dilatational phonon (see Fig. 7). This happens as a result of the fact that the zeroth mode makes only a small contribution to electron scattering. The increased significance

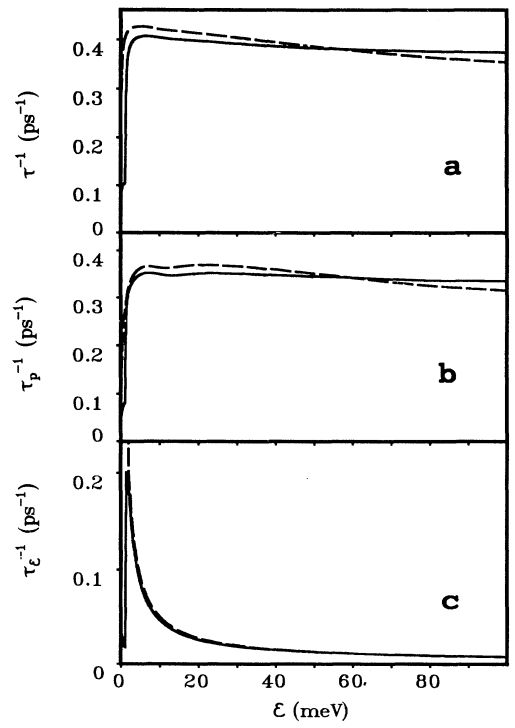


FIG. 8. The electron scattering rate, $\tau^{-1}$ (a), the inverse momentum relaxation time, $\tau_p^{-1}$ (b), and the inverse energy relaxation time, $\tau_\varepsilon^{-1}$ (c) as functions of electron energy. Degenerate electron gas, $\varepsilon_F = 50$ meV, $T = 300$ K, GaAs FSQW of width 100 Å. The solid lines correspond to acoustic phonon emission and the dashed lines correspond to acoustic phonon absorption.

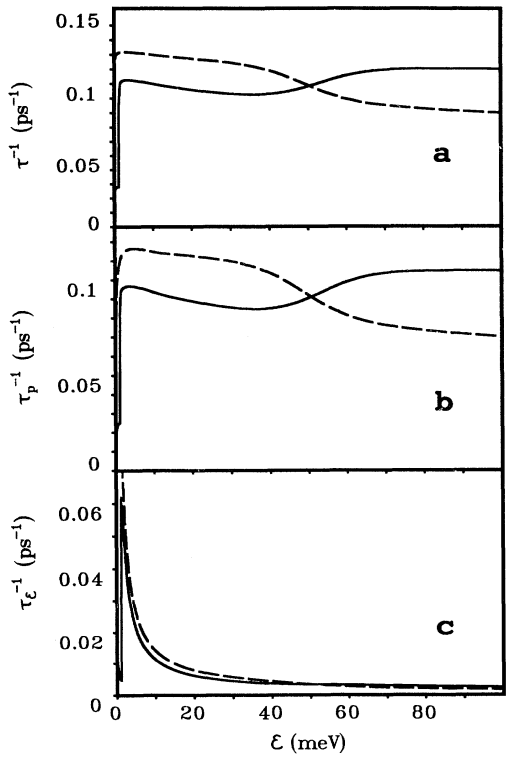


FIG. 9. The electron scattering rate, $\tau^{-1}$ (a), the inverse momentum relaxation time, $\tau_p^{-1}$ (b), and the inverse energy relaxation time, $\tau_\varepsilon^{-1}$ (c) as functions of electron energy. Degenerate electron gas, $\varepsilon_F = 50$ meV, $T = 300$ K, GaAs FSQW of width 100 Å. The solid lines correspond to acoustic phonon emission and the dashed lines correspond to acoustic phonon absorption.

of the first mode is related to the fact that the parameter $q_l$ for the zeroth mode is pure imaginary (see Fig. 1); therefore the Hamiltonian for the electron-phonon interactions has surface bound character [see Eq. (22)] and has a small overlap with electron wave function of the ground state. The modes of the order higher than one also have low interaction intensity with electrons because of more frequent spatial oscillation than in the first mode.

The relaxation times for the degenerate case look more complicated; however, their behavior will be quite clear if we analyze the factor $\mathcal{F} = (1 - f^0_{\mathbf{p}'})/(1 - f^0_{\mathbf{p}})$, which stands under the integral (or under the summation sign) in Eqs. (30), and (34)–(36), and distinguishes this case from the nondegenerate case. If $\varepsilon - \varepsilon_F \gg T$ and $\varepsilon' - \varepsilon_F \gg T$, then $\mathcal{F} \approx 1$. Thus, if the electron energies before scattering, $\varepsilon$, and after scattering, $\varepsilon'$, are slightly higher than the Fermi energy, the relaxation rates are the same as for the nondegenerate case. The energies $\varepsilon$ and $\varepsilon'$ are related by the equality $\mid \varepsilon - \varepsilon' \mid = \hbar\omega$, where $\hbar\omega$ is the energy of the emitted or absorbed acoustic phonon. So, the relaxation rates for the degenerate case coincide with the relaxation rates for the nondegenerate case for energies larger than the Fermi energy plus $\hbar\omega$ plus a few $T$.

For energies $\varepsilon - \varepsilon_F \ll T$, $\varepsilon' - \varepsilon_F \ll T$, the factor

$\mathcal{F} \approx \exp(\frac{\varepsilon'-\varepsilon}{T})$. The value of the factor $\mathcal{F}$ is different for phonon emission and phonon absorption. In the case of phonon emission $\mathcal{F} = \exp(-\hbar\omega/T)$ and in the case of phonon absorption $\mathcal{F} = \exp(\hbar\omega/T)$. The energy dependences of the relaxation rates for energies lower than the Fermi energy are basically the same as for domains of high energies; however, these pieces of graphs are multiplied by the factor $\mathcal{F} = \exp(-\hbar\omega/T)$ for the phonon emission and the factor $\mathcal{F} = \exp(\hbar\omega/T)$ for the phonon absorption.

If we take into account the fact that $\hbar\omega \approx 1$ meV for a GaAs FSQW of width 100 Å, the transition from the energies lower than $\varepsilon_F$ to the energies higher than $\varepsilon_F$ is very steep for the case of $T = 4.2$ K [$\exp(\hbar\omega/T) \approx 15.8$], smooth for the case of $T = 77$ K [$\exp(\hbar\omega/T) \approx 1.16$], and is practically invisible for the case of $T = 300$ K [$\exp(\hbar\omega/T) \approx 1.04$].

## V. KINETIC RELAXATION TIME

In this section we will use the kinetic approach to analyze the electron relaxation times. We restrict ourselves by the case where only the lowest electron subband is occupied. We will study the electron transport properties on the basis of solving the kinetic equation for electrons. In the case of a linear response of the electron gas to the applied external force $\mathbf{F}$ we may represent the electron distribution function in the form

$$f = f^0_{\mathbf{p}} + \frac{\mathbf{f}_{1p}\,\mathbf{p}}{p}, \tag{37}$$

where the function $\mathbf{f}_{1p}$ depends on the absolute value of the momentum, $\mathbf{p}$, and does not depend on the direction of $\mathbf{p}$.

Momentum $\mathbf{p}$ has polar coordinates $(p, \phi)$. If we multiply the kinetic equation for electron distribution function $f$ with collision integral (28) by $\mathbf{p}/p$ and integrate over the polar angle $\phi$, we obtain the following equation for $\mathbf{f}_{1p}$:

$$\mathbf{F}\frac{\partial f^0_{\mathbf{p}}}{\partial p} = \sum_{\mathbf{p}'} W_{\mathbf{p}\to\mathbf{p}'}\left[\frac{f^0_{\mathbf{p}}}{f^0_{\mathbf{p}'}}\,\mathbf{f}_{1p'}\cos\varphi - \frac{1-f^0_{\mathbf{p}'}}{1-f^0_{\mathbf{p}}}\,\mathbf{f}_{1p}\right]. \tag{38}$$

We are looking for the solution of Eq. (38) in the representation

$$\mathbf{f}_{1p} = -\tau_1(p)\,\mathbf{F}\frac{\partial f^0_{\mathbf{p}}}{\partial p}. \tag{39}$$

It follows from the consideration given below that $\tau_1(p)$ may be interpreted as a momentum relaxation time in the kinetic approximation (or kinetic relaxation time). From Eqs. (38) and (39) we may obtain the Fredholm equation of the second kind for the function $\tau_1(p)$,

$$\tau_1(p) = \tau(p) + \tau(p)\sum_{\mathbf{p}'} W_{\mathbf{p}\to\mathbf{p}'}\,\frac{p'\cos\varphi}{p} \times\tau_1(p')\,\frac{1-f^0_{\mathbf{p}'}}{1-f^0_{\mathbf{p}}}, \tag{40}$$

or the equivalent equation

$$\tau_1(p)^{-1} = \sum_{\mathbf{p}'} W_{\mathbf{p}\to\mathbf{p}'}\left[1 - \frac{p'\cos\varphi}{p}\,\frac{\tau_1(p')}{\tau_1(p)}\right]\frac{1-f^0_{\mathbf{p}'}}{1-f^0_{\mathbf{p}}}. \tag{41}$$

The equation for $\tau_1(p)$ in the form (41) differs from the formula (35) for the momentum relaxation time in the test-particle approximation only by factor $\tau_1(p')/\tau_1(p)$. This factor is equal to unity if the scattering is elastic, so in the elastic scattering approximation $\tau_1(p) = \tau_p(p)$. In general, we have to solve the Fredholm equation of the second kind.

The kinetic relaxation time is directly related to the electron mobility $\mu = e\tau_t/m^*$, where $\tau_t$ is the averaged kinetic relaxation time expressed by the formula

$$\tau_t = \frac{\int_0^\infty d\varepsilon\,(\varepsilon/T)\,\tau_1(\varepsilon)\,f^0_{\mathbf{p}}\,(1-f^0_{\mathbf{p}})}{\int_0^\infty d\varepsilon\,f^0_{\mathbf{p}}}.$$

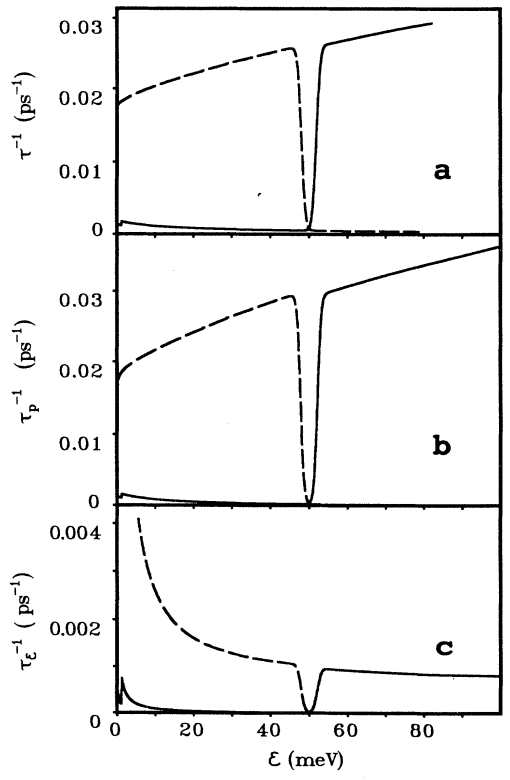


FIG. 10. The electron scattering rate, $\tau^{-1}$ (a), the inverse momentum relaxation time, $\tau_p^{-1}$ (b), and the inverse energy relaxation time, $\tau_\varepsilon^{-1}$ (c) as functions of electron energy. Degenerate electron gas, $\varepsilon_F = 50$ meV, $T = 300$ K, GaAs FSQW of width 100 Å. The solid lines correspond to acoustic phonon emission and the dashed lines correspond to acoustic phonon absorption.

We have solved the Fredholm equation (40) and Eq. (41) for function $\tau_1$ numerically by iterations taking $\tau_p$ as the initial approximation. The energy dependence of $\tau_1$ is similar to the energy dependencies of the momentum relaxation time, $\tau_p$, and inverse scattering rate, $\tau$, and, because of this, we do not give graphs for $\tau_1$.[41] The main conclusion we may derive from this similarity is that the relaxation times $\tau_p$ and $\tau$ are very good approximations for the evaluation of the electron transport properties due to the electron scattering by confined acoustic phonons.

## VI. SUMMARY

We have analyzed the confined acoustic modes in FSQW's. The dilatational and flexural modes may contain terms localized near the surface of the quantum well as well as terms propagating throughout the width of the quantum well. The lowest flexural mode is completely localized near the surface while the lowest dilatational mode is completely localized only if the in-plane wave vector is large enough. The higher order modes always have propagating terms. Localization near the surface is present for high values of the in-plane wave vectors. The Hamiltonian for electron-acoustic phonon interactions has symmetrical form for the case of the dilatational phonons and antisymmetric form for the case of the flexural phonons. Accordingly, if the potential energy for electrons in the quantum well is a symmetric function, so that the electron states may be classified by the symmetry of the electron wave functions into symmetric and antisymmetric states, then the dilatational phonons will interact only with electrons scattered between two states of the same symmetry while the scattering by the flexural phonons will result in the electron transition between two states of the opposite symmetry. We have calculated the rate of electron scattering by confined acoustic phonons and the corresponding relaxation times for the case of the infinitely deep quantum well for electrons. We have found that the first dilatational mode makes the main contribution to the electron-phonon scattering. The increased significance of the first mode is related to the fact that the Hamiltonian for electron-acoustic phonon interactions for the zeroth mode has surface-bound character, so its interaction with electrons is weakened. The modes of the order higher than one also have low interaction intensity with electrons because of more frequent spatial oscillations than in the first mode.

## ACKNOWLEDGMENTS

This work was supported by NSF and ARO.

[1] M. Grimsditch, R. Bhadra, and I. Schuller, Phys. Rev. Lett. **58**, 1216 (1987).
[2] B. Bhadra, M. Grimsditch, I. Schuller, and F. Nizzoli, Phys. Rev. B **39**, 12 456 (1989).
[3] M. D. Williams, S. C. Shunk, M. G. Young, D. P. Docter, D. M. Tennant, and B. I. Miller, Appl. Phys. Lett. **61**, 1353 (1992).
[4] A. K. Viswanath, K. Hiruma, M. Yazawa, K. Ogawa, and T. Katsuyama, Microw. Opt. Tech. Lett. **7**, 94 (1994).
[5] K. Yoh, A. Nishida, H. Kunitomo, T. Ogura, and M. Inoue, Jpn. J. Appl. Phys. **32**, 6237 (1993).
[6] K. Hiruma, M. Yazawa, K. Haraguchi, K. Ogawa, T. Katsuyama, M. Koguchi, and H. Kakibayashi, J. Appl. Phys. **74**, 3162 (1993).
[7] M. A. Foad, C. D. Wilkinson, C. Dunscomb, and R. H. Williams, Appl. Phys. Lett. **60**, 2531 (1992).
[8] K. Tsutsui, E. L. Hu, and C. Wilkinson, Jpn. J. Appl. Phys. **32**, 6233 (1993).
[9] L. T. Canham, Appl. Phys. Lett. **57**, 1046 (1990).
[10] T. Itoh and T. Suga, Jpn. J. Appl. Phys. **33**, 334 (1994).
[11] S. T. Ho, S. L. McCall, R. E. Slusher, L. N. Pheiffer, K. W. West, A. Levi, G. Blonder, and J. Jewell, Appl. Phys. Lett. **57**, 1387 (1990).
[12] T. S. Ravi and R. B. Marcus, J. Vac. Sci. Technol. B **9**, 2733 (1991).
[13] G. D. Sanders and Y. C. Chang, Appl. Phys. Lett. **60**, 2525 (1992).
[14] G. D. Sanders, C. J. Stanton, and Y. C. Chang, Phys. Rev. B **48**, 11 067 (1993).
[15] Y. F. Chen, J. L. Chen, L. Y. Lin, and Y. S. Huang, J. Appl. Phys. **73**, 4555 (1993).
[16] J. C. Nabity and M. N. Wybourne, Phys. Rev. B **44**, 8990 (1991).
[17] J. Seyler and M. N. Wybourne, Phys. Rev. Lett. **69**, 1427 (1992).
[18] L. J. Challis, A. J. Kent, and V. W. Rampton, Semicond. Sci. Technol. **5**, 1179 (1990).
[19] M. Rosenfusser, L. Koster, and W. Dietsche, Phys. Rev. B **34**, 5518 (1986).
[20] H.-N. Lin, H. J. Maris, and L. B. Freund, J. Appl. Phys. **73**, 37 (1993).
[21] *Physical Acoustics*, edited by W. Mason (Academic Press, New York, 1964), Vol. 1, Part A.
[22] B. A. Auld, *Acoustic Fields and Waves* (Wiley, New York, 1973).
[23] L. Wendler and V. G. Grigoryan, Surf. Sci. **213**, 588 (1989).
[24] L. Wendler and V. G. Grigoryan, Phys. Rev. B **42**, 1833 (1990).
[25] B. Sylla, M. More, and L. Dobrzynski, Surf. Sci. **206**, 203 (1988).
[26] V. Velasko and B. Djafari-Rouhani, Phys. Rev. B **26**, 1929 (1982).
[27] A. Akjouj, B. Sulla, P. Zielinski, and L. Dobrzynski, J. Phys. C **20**, 6137 (1987).
[28] V. Velasko and F. Garcia-Moliner, Phys. Scr. **20**, 111 (1979).
[29] V. A. Kochelap and O. Gulseren, J. Phys. Condens. Matter **5**, 589 (1993).
[30] A. Kosevich and V. Khokhlov, Sov. Phys. Solid State **10**, 39 (1968).
[31] M. A. Stroscio and K. W. Kim, Phys. Rev. B **48**, 1936 (1993).

[32] M. Stroscio, G. Iafrate, K. Kim, V. Mitin, and N. Bannov, in *Proceedings of the 1993 International Semiconductor Device Research Symposium*, edited by M. Shur (Academic Outreach, Charlottesville, 1993), p. 873.
[33] V. G. Grigoryan and D. E. Sedrakyan, Sov. Phys. Acoust. **29**, 281 (1983).
[34] N. Bannov, V. Mitin, and M. A. Stroscio, Phys. Status Solidi B **183**, 131 (1994).
[35] N. Bannov, V. Mitin, and M. Stroscio, in *Proceedings of the 1993 International Semiconductor Device Research Symposium* (Ref. 32), p. 659.
[36] K. W. Kim, SeGi Yu, M. U. Erdoğan, M. A. Stroscio, and G. J. Iafrate, SPIE Proc. **2142**, 77 (1994).
[37] R. W. Morse, J. Acoust. Soc. Am. **22**, 219 (1950).
[38] C. Lanczos, *The Variational Principles of Mechanics* (University of Toronto Press, Toronto, 1964).
[39] G. L. Bir and G. E. Pikus, *Symmetry and Strain-Induces Effects in Semiconductors* (John Wiley and Sons, New York, 1974).
[40] L. Wendler, Phys. Status Solidi, **129**, 513 (1985); **141**, 129 (1987).
[41] This is exactly so for $T = 77$ K and for $T = 300$ K. For $T = 4.2$ K the graphs for $\tau_1(\varepsilon)$ have fine structures imposed on the smooth dependences which are similar to the dependences of $\tau(\varepsilon)$ and $\tau_p(\varepsilon)$. For more details see N. Bannov, V. Aristov, and V. Mitin, Solid State Commun. **93**, 483 (1995).